ELSEVIER

Palaeogeography, Palaeoclimatology, Palaeoecology 169 (2001) 113–127

PALAEO

www.elsevier.nl/locate/palaeo

Hydrological modelling of a Pleistocene landslide-dammed lake in the Santa Maria Basin, NW Argentina

Bodo Bookhagen*, Kirk Haselton, Martin H. Trauth

Institut für Geowissenschaften, Universität Potsdam, Postfach 601553, D-14415 Potsdam, Germany

Received 14 December 1999; accepted for publication 26 January 2001

Abstract

Around 30,000 ^{14}C yr BP, multiple landslides in the Quebrada de Cafayate (26°S, 66°W) dammed the Río de las Conchas and caused a lake in the Santa Maria Basin, NW Argentina. Since climate could have played a major role in landslide generation, we used a lake-balance model to compare the present-day climate with the conditions during landsliding. This model reveals that a hypothetical present-day lake would stabilize around 70 m below the reconstructed paleolake level. The volume of the water body would be one third of the corresponding paleolake volume. However, a minimum 10–15% increase in mean-annual precipitation accompanied by at least a 3–4°C drop in temperature would result in a stable lake level at the reconstructed elevation. This result implies wetter and cooler conditions at 30,000 ^{14}C yr BP as compared to the present. Wetter climate in turn could help to explain enhanced landsliding in the Quebrada de Cafayate during this time.

Keywords: South America; Paleoclimate; Modelling; Quaternary

1. Introduction

Climate has been identified as a major influential factor for landsliding in mountainous regions (e.g. Dethier and Reneau, 1996; Reneau and Dethier, 1996). Increased humidity can cause enhanced scouring, undercutting and higher pore-water pressure of structurally pre-conditioned mountain fronts and valley walls. When landsliding in narrow river valleys causes damming of streams, the resultant lake deposits may potentially provide information on paleoclimatic conditions during landsliding. Landslide deposits and associated lake deposits can help to assess the role of climate on landsliding in such a region.

Numerous landslide-dammed paleolakes in the northwest Argentine Andes occurred at around 30,000 ^{14}C yr BP (Hermanns and Strecker, 1999; Trauth and Strecker, 1999; Hermannes et al., 2000; Trauth et al., 2000). The most prominent example is the paleolake that formed in the Santa Maria Basin after multiple landsliding in the Quebrada de Cafayate at 30,000 ^{14}C yr BP (Fig. 1). As inferred from the lake deposits, this freshwater lake reached a maximum elevation of 1700 m a.s.l. and covered an area of 658 km^2. This landslide cluster corresponds to the Minchin wet period (between ca. 40,000 and 25,000 ^{14}C yr BP) reported from other places in subtropical and tropical South America (van der Hammen, 1994; Wirrmann and Mourguiart, 1995; Ledru et al., 1996; Turcq et al., 1997). However, no paleoclimate data exist for the Santa Maria Basin.

The atmospheric circulation of northwestern

* Corresponding author. Fax: +49-331-977-2087.
E-mail address: bodo@geo.uni-potsdam.de (B. Bookhagen).

0031-0182/01/$ - see front matter
PII: S0031-0182(01)00221-8

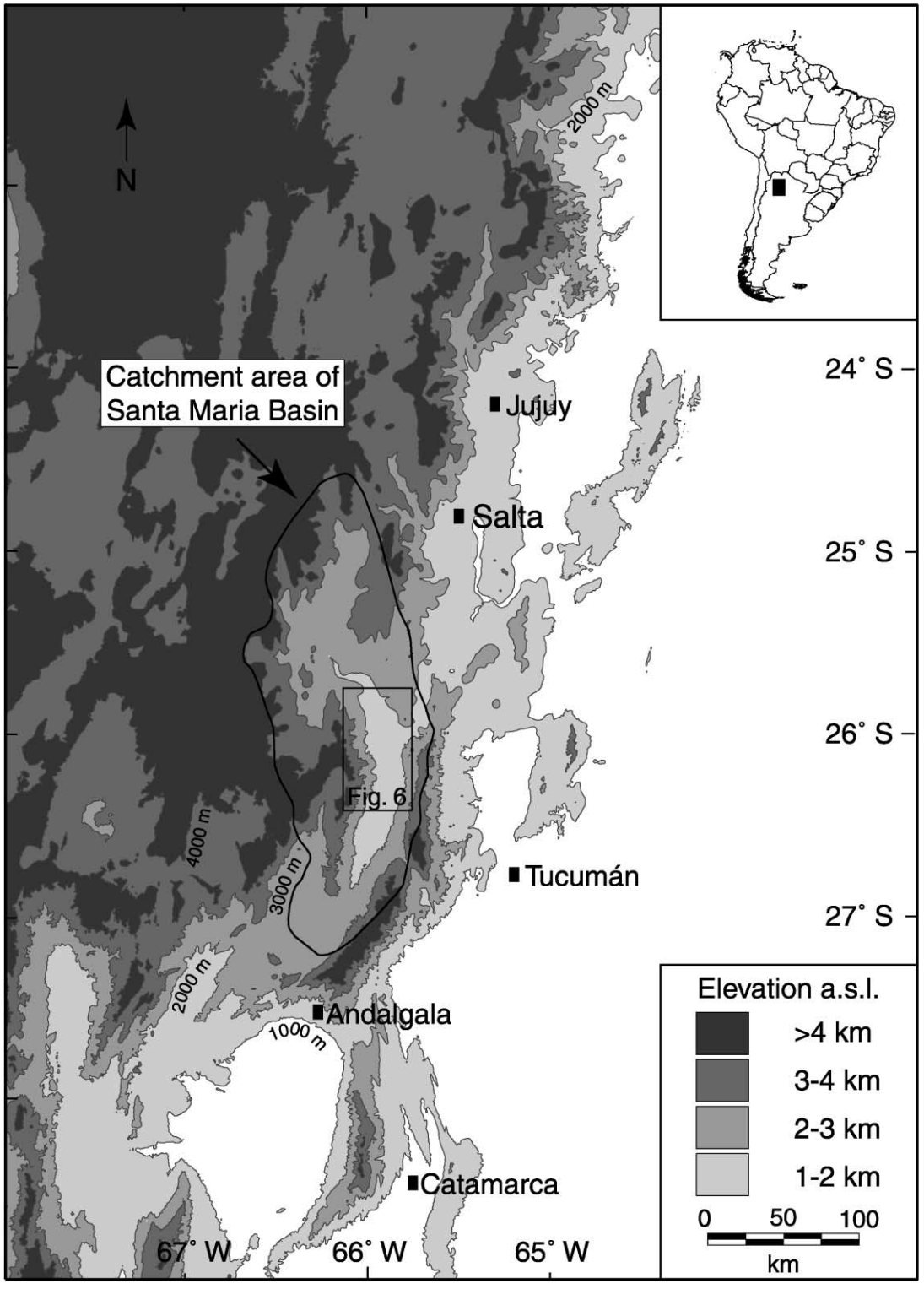
N
2000 m
Catchment area of
Santa Maria Basin
Jujuy
Salta
Fig. 6
4000 m
3000 m
Tucumán
2000 m
1000 m
Andalgala
Catamarca
24° S
25° S
26° S
27° S
67° W
66° W
65° W
Elevation a.s.l.
>4 km
3-4 km
2-3 km
1-2 km
0
50
100
km

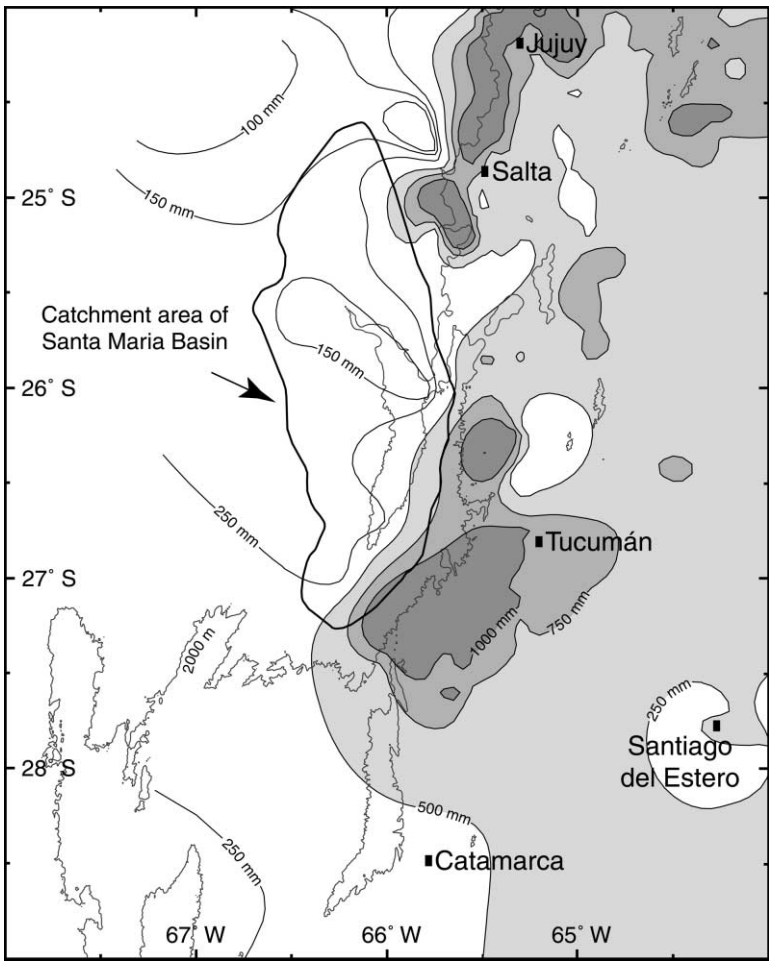

Fig. 2. Mean-annual precipitation in NW Argentina showing maxima along the eastern slopes of the ranges in Tucumán, Salta and Jujuy. The intra-Andean region receives less than 20% of the precipitation value east of the mountains due to orographic rain-shadow effects. Averaged mean-annual precipitation over the outlined catchment area of the Santa Maria Basin is 250 mm yr^{-1} (raw precipitation data from Bianchi and Yañez, 1992).

Argentina is characterized by northeasterly and easterly moisture-bearing winds that develop in response to a seasonal low-pressure system east of the Andes. The low-pressure cell also attracts air masses from the Pacific anticyclone creating a dry and cold wind that gains intensity during the austral winter (Prohaska, 1976; Hastenrath, 1991). Precipitation within the study area is highly seasonal. Summer precipitation is associated with convection and winter precipitation with equatorward moving cold fronts (Lenters and Cook, 1999). Orographic precipitation exceeding 1500 mm yr^{-1} from the dominant easterly and northeasterly winds is produced along the high, steep eastern slopes of the north–south oriented Andean ridges. The arid intra-Andean basins and valleys receive less than 200 mm yr^{-1} precipitation which results in a sparse vegetation cover (Fig. 2) (Galvan, 1981; Bianchi and Yañez, 1992). Climate stations report a range of persistent moist summer wind directions from southwesterly (Tucumán) to northeasterly (Salta),

Fig. 1. Topographic map of NW Argentina showing the catchment area of the Santa Maria Basin (contours in meters above sea level).

with dry northerlies common at both localities during the winter (Prohaska, 1976).

In order to investigate the paleoclimatic situation during landsliding and lake development, we applied a lake-balance model which links climate and hydrology in closed-basin lakes. The model simulates a lake, which would develop after closure of the Quebrada de Cafayate in the location of the fossil landslide deposits, determining an equilibrium lake level for the present-day climate. The values of precipitation and temperature are then changed in a way that the equilibrium lake level adjusts to the 1700 m contour line, simulating climate conditions at the time of paleolake occurrence about 30,000 ^{14}C yr ago. The differences between the present-day and past climatic setting are discussed as a potential explanation for enhanced landsliding 30,000 ^{14}C yr ago in a region without such landsliding activity today.

2. The model

Lake-balance models compute an equilibrium lake level for closed-basin lakes using the balance between basin-averaged precipitation and evaporation. Whereas the value for precipitation P is in principle easy to measure, evaporation E is extremely difficult to estimate. In most cases, E is calculated using empirical equations incorporating the environmental setting and climatic parameters such as temperature, relative humidity, windspeed and cloud coverage. Two different modelling approaches are commonly used for estimating evaporation with respect to atmospheric conditions, the energy-budget and bulk-transfer methods. The energy budget method evaluates the incoming and outgoing radiation at the earth's surface. The bulk transfer method parameterizes evaporation in terms of windspeed and surface characteristics.

3. Algorithm

Hastenrath and Kutzbach (1985) provide a conceptual but simplified framework for the water and energy budget of Lake Titicaca balancing basin-averaged precipitation P_{bas} and evaporation E_{bas} (Eq. (1)). The steady-state hydrologic budget for a closed basin is governed by the evaporation from the water and land surface and the precipitation in the catchment area (Hastenrath and Kutzbach, 1985):

$$P_{bas} = E_w a_w + E_l(1 - a_w) = E_{bas} \quad (1)$$

where E_w and E_l denote the evaporation over water and land, respectively, and a_w is the lake-area ratio, the fraction of the catchment area's surface covered by water. For example, Kessler (1984) introduced a bulk-transfer formula to estimate the sensitivity of Altiplano evaporation rates E to changes in only two parameters, temperature and relative humidity. However, Kessler's model makes the simplifying assumption that the surface temperature of the lake and the local air temperature are the same, which is not true for the modern case and may be even more inappropriate for past conditions. Additionally, the evaporation depends not only on the absolute value of the air temperature but is also highly influenced by the gradient between the temperature T_a usually obtained 2 m above the ground and the temperature T_s measured right above the surface. Hastenrath and Kutzbach (1985) estimated evaporation rates on the Altiplano, assuming identical surface and air temperatures and concluded that evaporation is relatively insensitive to changes in temperature, relative humidity and cloudiness. Again, the surface temperature and air temperature were taken to be identical. Blodgett et al. (1997) introduced an improved lake-balance model taking into account the dependency of E on this temperature gradient, where T_a is obtained from standard climate datasets and T_s is computed by an improved energy budget method, which incorporates separately the radiation components. This energy budget method is based on the fact that the net heating rate, i.e. the difference between incoming and outgoing radiation at the earth surface, is zero (Brutsaert, 1982; Shuttleworth, 1988):

$$R_{sw} - R_{lu} + \epsilon \cdot R_{ld} - H - L \cdot E = 0 \quad (2)$$

where R_{sw} is the net short wave radiation down, R_{lu} the long wave radiation up, ϵ the surface emissivity, R_{ld} the long wave radiation down, H the sensible heating rate, L the latent heat of vaporization and E is the evaporation. Herein, R_{sw} is calculated from the cloud free short wave radiation R_{swc}, the surface albedo α, two values referring to short wave cloud parameters a

Table 1
List of all parameters which are used in the bulk transfer and energy budget methods

Parameter	Units	Modern value[a]	Paleo value[b]	Description	Ref.
A_w	km^2	379	658	Lake area, part of the basin covered by water	[c]
a_w	–	0.017	0.030	Lake-area ratio, fraction of the basin's surface area covered by water	[c]
V_w	km^3	22.9	61.8	Volume of the lake water body	[c]
P_{bas}	mm a^{-1}	250	275	Basin-averaged precipitation rate	[d]
E_{bas}	mm a^{-1}	237	264	Basin-averaged evaporation rate	[e]
T_s	°C	20.4[f], 19.0[g]	16.1[g]	Surface temperature	
T_a	°C	9.5[h]	6.5	Air temperature	
C_D	–	1.1×10^{-3}	1.5×10^{-3}	Surface-drag coefficient over land	[i]
C_D	–	7.3×10^{-4}		Surface-drag coefficient over water	[i]
A_d	km^2	21,970		Area of the catchment basin	[c]
$es(T)$	Pa	x[j]		Saturation vapor pressure at a given air temperature T_a	
P	Pa	1.27×10^5		Air pressure	[k]
U	m s^{-1}	3.60		Windspeed	[k]
cc	–	0.43		Cloud fraction	[k]
rh	–	0.30		Relative humidity	[k]
α_w, α_l	–	0.085, 0.200		Surface albedo over water, land	[l]
ϵ_w, ϵ_l	–	0.97, 0.85		Surface emissivity over water, land	[l]
f_w,f_l	–	1.0, 0.1		Soil moisture or moisture availability function over water, land	[l]
a,b	–	0.39, 0.38		Shortwave cloud parameters	[l]
a', b'	–	0.22, 2.0		Long wave clound parameters	[l]
D	mm a^{-1} m^{-2}	9.33		Basin drainage	[m]
λ	–	0.017		Runoff-coefficient reflecting precipitation lost to the ground	[n]
R_{swc}	W m^{-2}	375.2		Cloudfree shortwave radiation	

[a] Modern value refers to hypothetical lake surface at the 1630 m a.s.l. contour line.
[b] Paleo value refers to the paleolake surface at 1700 m a.s.l. contour line.
[c] Value taken from DEM.
[d] Bianchi and Yañez (1992).
[e] Bulk transfer method, using Eqs. (7) and (1).
[f] van Wambeke (1981).
[g] Modelled by energy budget method.
[h] Hoffmann (1975).
[i] See calibration section.
[j] Varies with temperature and is independent from setting.
[k] Salta Airport.
[l] Bougeault (1988).
[m] Malamud et al. (1996).
[n] This paper: sensitivity section.

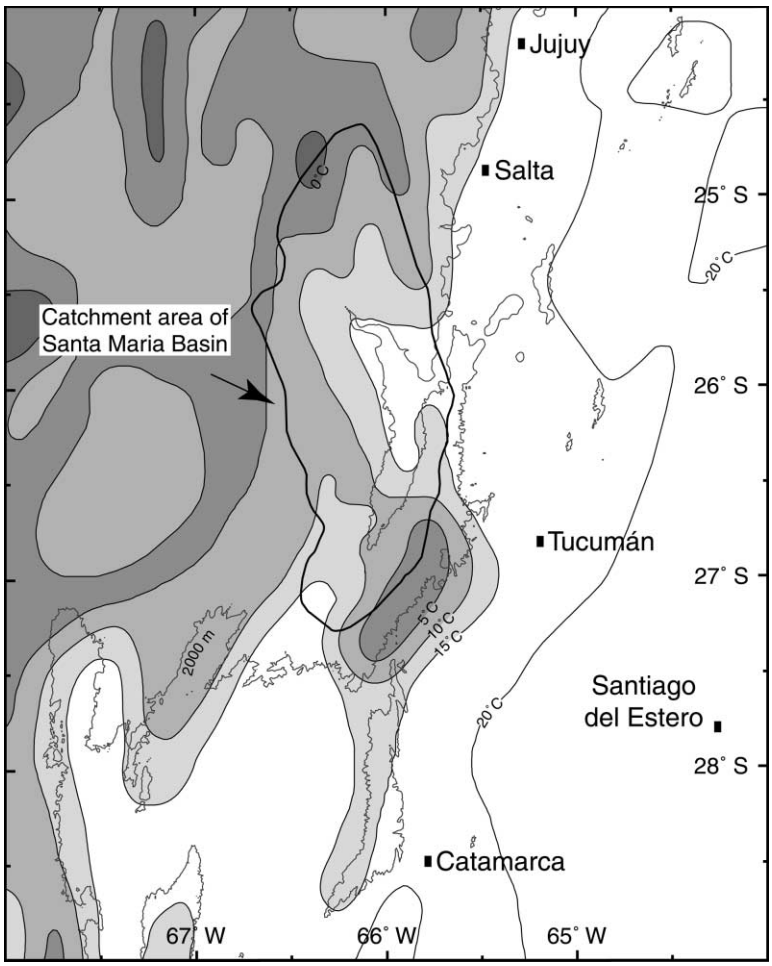

Fig. 3. Mean-annual temperature in NW Argentina mainly controlled by topography (Hoffmann, 1975). In the center part of the Santa Maria Basin, the wind influence from the east through the valleys is an additional factor controlling temperature.

and b and the cloud cover cc (Shuttleworth, 1988)

$$R_{sw} = R_{swc}(1 - \alpha)[1 - t(a + b{\cdot}cc)cc] \quad (3)$$

the net long wave radiation up R_{lu} is computed from the surface emissivity ϵ, the Stefan–Boltzmann constant σ and the surface temperature T_s

$$R_{lu} = \epsilon{\cdot}\sigma{\cdot}T_s^4 \quad (4)$$

The net long wave radiation down R_{ld} is obtained by

$$R_{ld} = 1.24\left[\frac{rh{\cdot}es(T_a)}{100T_a}\right]^{\frac{1}{7}}\sigma T_s^4(1 + a' \cdot cc^{b'})$$

where rh is the relative humidity, $es(T)$ the saturation vapour pressure depending on temperature, a' and b' refer to long wave cloud parameters. The value of the sensible heating rate H depends on the air pressure p, the surface-drag coefficient C_D, the windspeed U, the specific heat of dry air c_p, the gas constant for dry air R, the air and surface temperature T_a and T_s, respectively:

$$H = \frac{p{\cdot}C_D{\cdot}U{\cdot}c_p}{R{\cdot}T_a}(T_s - T_a) \quad (6)$$

The second method for calculating evaporation E,

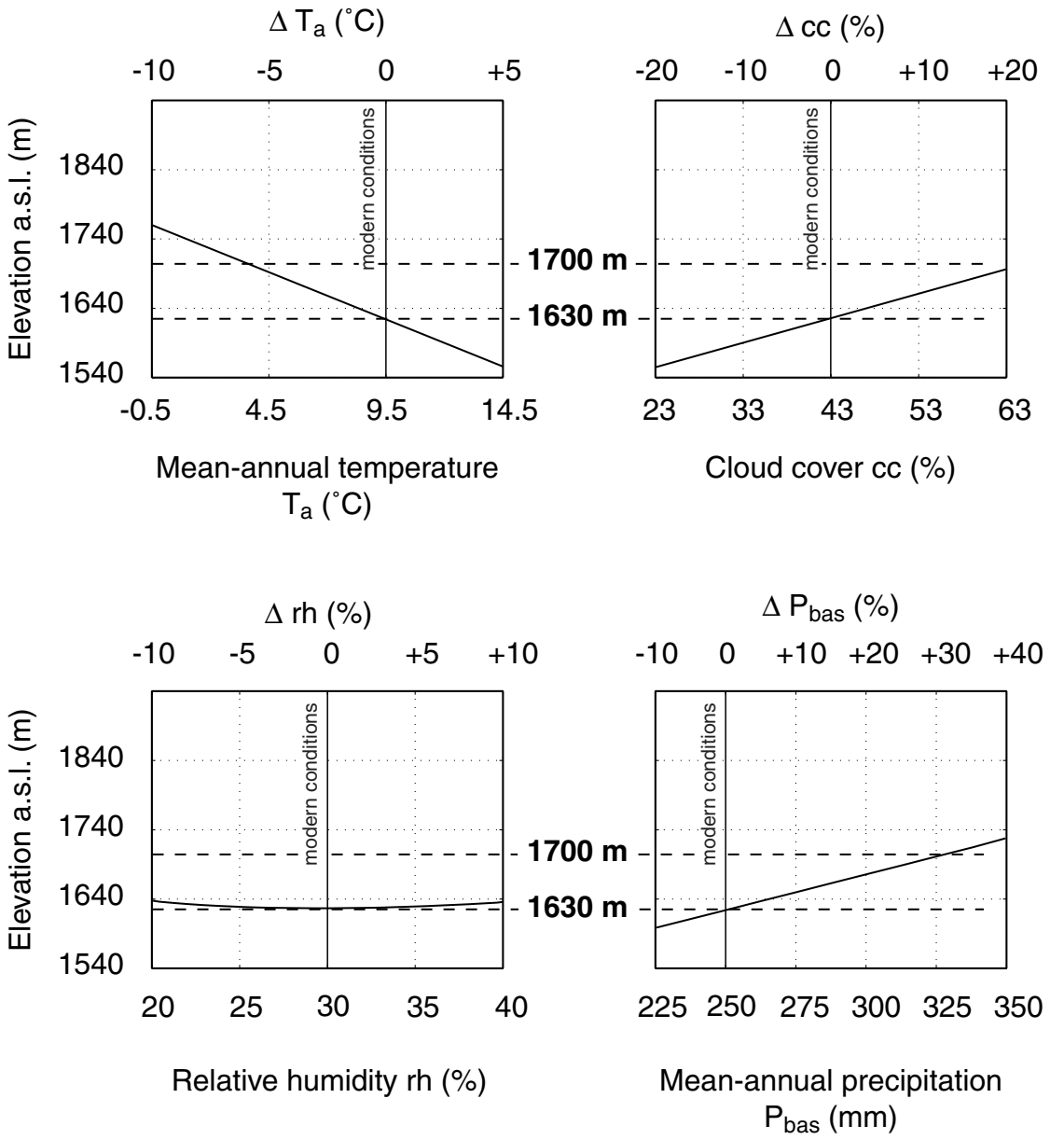

Fig. 4. Results of sensitivity tests (see text for further explanation). Change of lake level vs. changes in: (a) air temperature T_a with a recalculated surface temperature T_s, (b) cloud fraction cc, (c) relative humidity rh and (d) basin averaged precipitation P_{bas}. The model output is mainly controlled by temperature and precipitation changes, whereas only unrealistic cloud cover and relative humidity changes cause significantly higher lake levels.

bulk transfer, is described by (Brutsaert, 1982):

$$E = \frac{0.622 C_D \cdot U \cdot f}{R \cdot T_a} [\mathrm{es}(T_s) - \mathrm{rh} \cdot \mathrm{es}(T_a)] \quad (7)$$

where f is the moisture availability function (for parameter information see Table 1).

In contrast to the basin-averaged models by Hastenrath and Kutzbach (1985), Kessler (1984), Blodgett et

al. (1997), we computed the hydrological budget for a catchment area with spatially varying values for P, T_a, T_s, p, α and ϵ. Since the precipitation P, the temperature T and the elevation-dependant pressure p varies widely over the catchment area (Figs. 1–3), the basin averaged values would not account for the spatial heterogeneity. Additionally the geologic (lithologic) differences in the catchment area are compensated by a separate calculation for albedo α and emissivity ϵ (Bougeault, 1988). Herein, the surface geology has been determined by available geologic maps and a Landsat-TM image classification. Therefore, all spatially varying climatological datasets were resampled to a common $0.05 \times 0.05°$ regular grid (approximately 5.6 km in square) using t-spline interpolation techniques (Wessel and Bercovici, 1998). The hydrologic budget for each cell has been calculated separately to account for the spatial inhomogeneity. A simple summation of all cells gives a basin-averaged value. We explicitly chose those variables (P, T_a, T_s, p, α and ϵ), because (a) they can easily be interpolated without introducing large uncertainties, (b) P and T show the greatest influence on model results and (c) they vary spatially even over this small basin (whereas cloud cover does not vary appreciably over the basin). All spatial calculations concerning the catchment area and the water body are based on a digital elevation model (DEM) compiled from maps at a scale of 1:250,000 and 1:25,000. This DEM was compared with the independent GTOPO30 dataset provided by the US Geological Survey's EROS Data Center in Sioux Falls, South Dakota. The difference between the two DEM's in the calculated areas and volumes is very small (less than 2%).

4. Parameterizations and calibration

Our two-dimensional raster-based model is computed for about 800 grid cells covering approximately 5.6 km in square, and contains various types of information including: precipitation P, air temperature T_a, surface temperature T_s, air pressure p, albedo α depending on lithology, surface emissivity ϵ, surface-drag coefficient C_D with two different values for water vs. dry ground and a regional moisture availability function f, again with different values for water and land (Bougeault, 1988).

First, the surface-drag coefficient C_D over land has to be determined. C_D remains constant for each run of the model and depends on the ratio of the reference height z_r to the roughness height z_0:

$$C_D = \kappa^2 \cdot \ln\left(\frac{z_r}{z_0}\right)^{-2} \quad (8)$$

where the Karman constant κ has a value of $\kappa = 0.40$ (Hartmann, 1994). The reference height z_r is the elevation where the wind speed is measured. It can be taken at any level within the surface where the logarithmic profile is a good approximation of the actual flow. Assuming an average windspeed of 3.6 m s^{-1} at two meters above the ground for the Santa Maria Basin (Table 1), the reference height has a value of $z_r = 162.5$ m (Rowntree, 1988). The roughness height z_0 is the height at which the windspeed reaches zero. The lowest z_0 for snow-free land surfaces applies to deserts, with values as low as $z_0 = 10^{-3}$ m resulting in $C_D = 1.1 \times 10^{-3}$. This value is a good estimate for arid regions (Rowntree, 1988). In contrast to the modern value, C_D over land may be slightly different for the paleoenvironment. Pollen analyses indicate a forest for parts of the catchment area at 30,000 ^{14}C yr BP (F. Schäbitz, personal communication 1998). Therefore, a slightly higher value of $C_D = 1.5 \times 10^{-3}$ was used based on $z_0 = 6 \times 10^{-3}$ m, keeping z_r and therefore the windspeed at the same value as before. These values are characteristic for such mixed environments (Hartmann, 1994; Rowntree, 1988). However, both values for C_D are within the typical range of $1–2 \times 10^{-3}$ for arid regions (Imberger and Patterson, 1990). For the calculation of C_D over water, z_0 is set to $z_0 = 6 \times 10^{-5}$ m, giving a $C_D = 7.3 \times 10^{-4}$ (Shuttleworth, 1993). The C_D over water is assumed to be constant through time.

Second, a value for the moisture availability function over land f_l has to be determined. This parameter varies from $f_l = 0$ for dry ground to $f_w = 1$ for water. In the Santa Maria catchment area the moisture availability function f_l varies roughly according to lithology and has an average value of $f_l = 0.1$. This average value is based on a weighted average of lithology-specific f_l values (Bougeault, 1988) determined from geologic maps and a classification of a Landsat-TM scene.

For the study area, the spatial distribution of

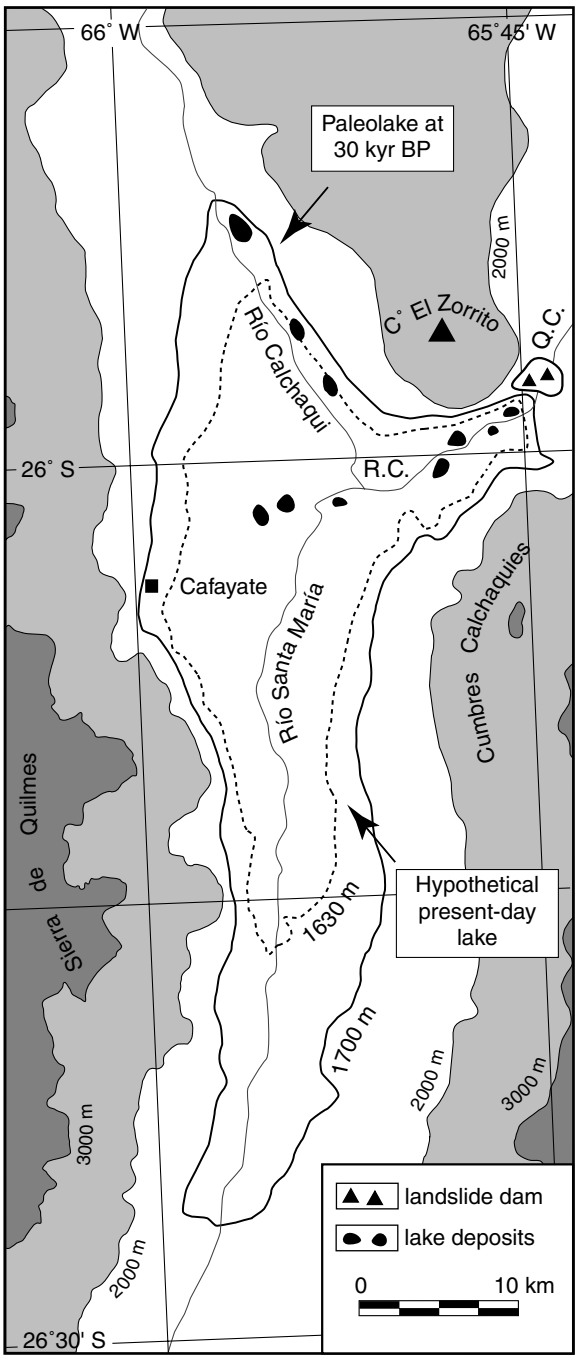

precipitation P was interpolated from the annual means for 380 irregularly-distributed stations in NW Argentina (Bianchi and yañez, 1992) (Fig. 2). Air temperature T_a is obtained by digitizing contour lines from the Climatic Atlas of South America (Hoffmann, 1975) (Fig. 3) and interpolating the data to the same grid as P. As described before, the surface temperature T_s (over land and water) is derived from the model by applying the combination of bulk transfer and energy budget methods in estimating evaporation. The cloud cover *cc* is from satellite ISCCP data, which covers most of the intraandean Santa Maria Basin. Relative humidity *rh* is taken from an area-averaged value for several towns in the vicinity of the Santa Maria Basin: Salta, Tucumán, Andalgala, La Rioja, Catamarca (Prohaska, 1976). The value for *cc* is in the same range as daily measurements at Salta Airport. The windspeed U, which was also taken from measurements at Salta Airport, is assumed to be constant over the whole basin. The variation of the Milankovitch-corrected solar radiation and its reflectance used in the energy budget equation is small during the 7000 yr long history of the lake at around 30,000 ^{14}C yr BP and are assumed to be constant (Berger and Loutre, 1991). Additional, short- and long-wave cloud parameters are taken from Shuttleworth (1988). The maximum paleolake level of 1700 m a.s.l. was inferred from the highest outcrops of lake sediments in the Santa Maria Basin (Trauth and Strecker, 1999) (Fig. 5). Diatom assemblages and the absence of evaporitic layers indicate prevailing freshwater conditions of the lake. After around 7000 yr, the termination of the lake was caused by erosion of the landslide dam after gradual filling of the basin with clastic deposits (Trauth and Strecker, 1999). During the existence of the lake the water level apparently never reached the top of the landslide dam at 1750 m a.s.l. (Hermanns and Strecker, 1999).

Based on the DEM, the reconstructed paleolake area is 658 km^2. The corresponding water body has a volume of 62 km^3 (Fig. 6). The difference between paleo-bathymetry and present-day topography subjected to erosional processes since 30,000 ^{14}C yr BP is small compared to the modelled fluctuations in

Fig. 5. Comparison of the hypothetical present-day lake and the paleolake at 30,000 ^{14}C yr BP in the Santa Maria Basin. The dashed line marks the 1630 m a.s.l. contour level for the hypothetical present-day lake as inferred from the lake-balance model for present-day climate conditions. The solid line shows the minimum paleolake extensions at 30,000 ^{14}C yr BP with an elevation of 1700 m a.s.l. as inferred from lake deposits. R.C. = Río de las Conchas, Q.C. = Quebrada de Cafayate.

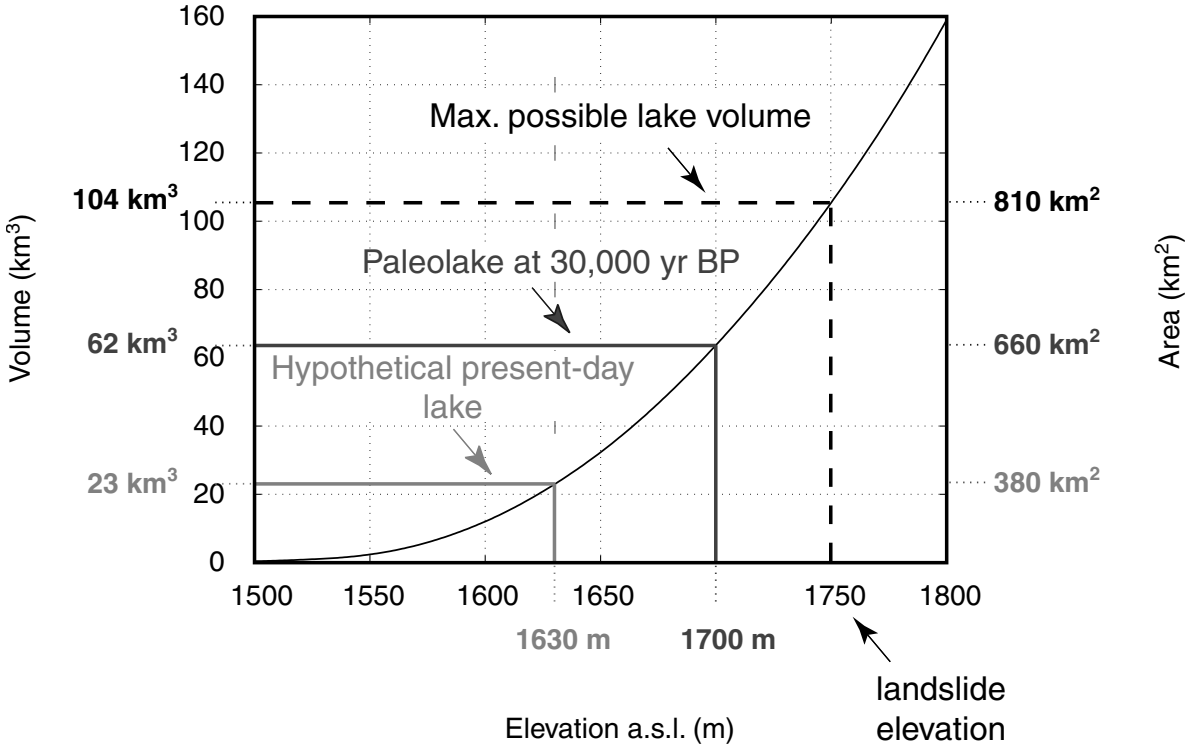

Fig. 6. Hypsometric curve derived from the digital elevation model (DEM) of the Santa Maria Basin. The modelled hypothetical present-day lake would have a volume of 23 km^3. In contrast, the paleolake at 30,000 ^{14}C yr BP had a water body in excess of 62 km^3. The basin volume constraint by the elevation of the landslide dam defines the maximum possible lake volume without overflow.

lake volume. The area of the drainage basin or the topography of the paleolake floor did not change significantly during the last 30,000 ^{14}C yr due to the erosion-resistant basin boundaries (Paleozoic granites and low-grade metamorphic rocks). The erosional volume below the lowest elevation of lake-sediment outcrops is calculated to be only a few percent of the overall basin volume. Therefore, the basin volume is not significantly influenced by erosion since the lake filled in and ceased to exist.

Since losses through the paleo-landslide dam or to groundwater cannot be completely ruled out, we take the calculated temperature T and precipitation P changes as minimum changes. P could have increased and T could have decreased even more. Still, it is a reasonable assumption to model a closed basin because: (a) the landslide dam had a higher elevation than the paleolake as inferred from lake sediments, (b) the landslide-dam deposits consist out of poorly-sorted material characterized by low porosity and permeability and (c) groundwater losses through the ground is very low due to the high clay content in the underlaying basin sediments (Tineo et al., 1993). Assuming a 10% loss of the inflow either through the dam or to groundwater, the resulting modelled temperature and precipitation change is negligible. It would decrease the value of evaporation by less than 0.5%. The important factor is that the equilibrium paleolake level stabilized well below the height of the landslide dam, so we assume there has been no overflow.

5. Sensitivity

The evaporation model contains four empirically-derived parameters that introduce some degree of uncertainty to the model results. Therefore, the model was intensely tested for its sensitivity to these parameters: air temperature depression dT_a, cloud

Table 2
Sensitivity table showing the change in evaporation ΔE (over both land and water) while increasing a given parameter by 10%. For parameter information see Table 1

Parameter	ΔE in (%)
a	−3
a'	+0.5
b	−1
b'	−1
U	3
cc	−4
rh	± 0
T_a	+5.5
λ	−0.5
a_w	+1.5

fraction increase *dcc*, relative humidity increase drh and percent-precipitation increase dP. To test the sensitivity of the model to the these parameters we calculated, one at a time, dT_a, d*cc*, d*rh* and dP that would be required to maintain a lake area ratio of $a_w = 0.03$ corresponding to a paleolake level at 1700 m a.s.l. (Fig. 4). In each test, one of the parameters was changed, the model was run and a resulting equilibrium lake level obtained, keeping the other three parameters fixed. These tests indicate that air temperature and basin-averaged precipitation rate are the most influential factors on the final result. Cloud cover affect model results, but not in a way as P and T do. Changes in relative humidity are of minor importance on the hydrologic balance of the modelled lake. Changes in windspeed U mainly affect evaporation but not the radiation balance and therefore are of lesser importance compared to the other parameters (see Table 2).

As second test, we increased all parameters by 10%, one at a time (Table 2). This test reveals that the result is relatively insensitive to changes of single parameters. Both tests suggest that significant changes of the hydrologic budget are most likely caused by combined changes of T and P.

Third, the quality of the final modelling result was evaluated by comparing the values of modelled parameters with observational data. As an example, the calculated mean-annual surface temperature of $T_s =$ 19.0°C for the basin is in good agreement with a value

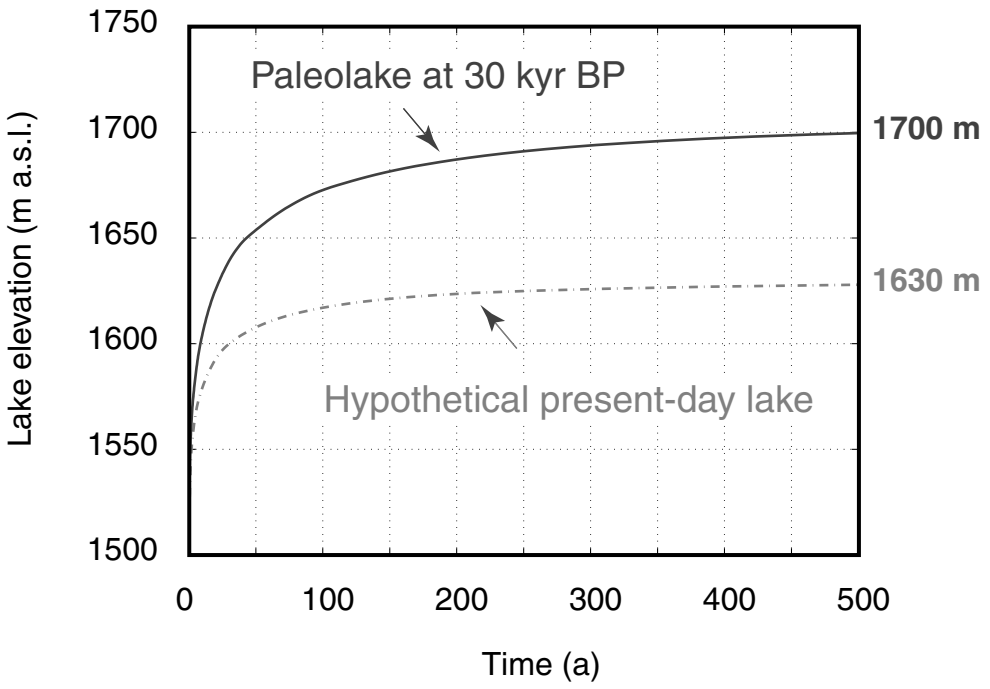

Fig. 7. Lake-fill curves for both the hypothetical present-day lake reaching the 1630 m contour and the paleolake produced by combined T and P changes in order to reach the 1700 m contour as reconstructed from lake deposits.

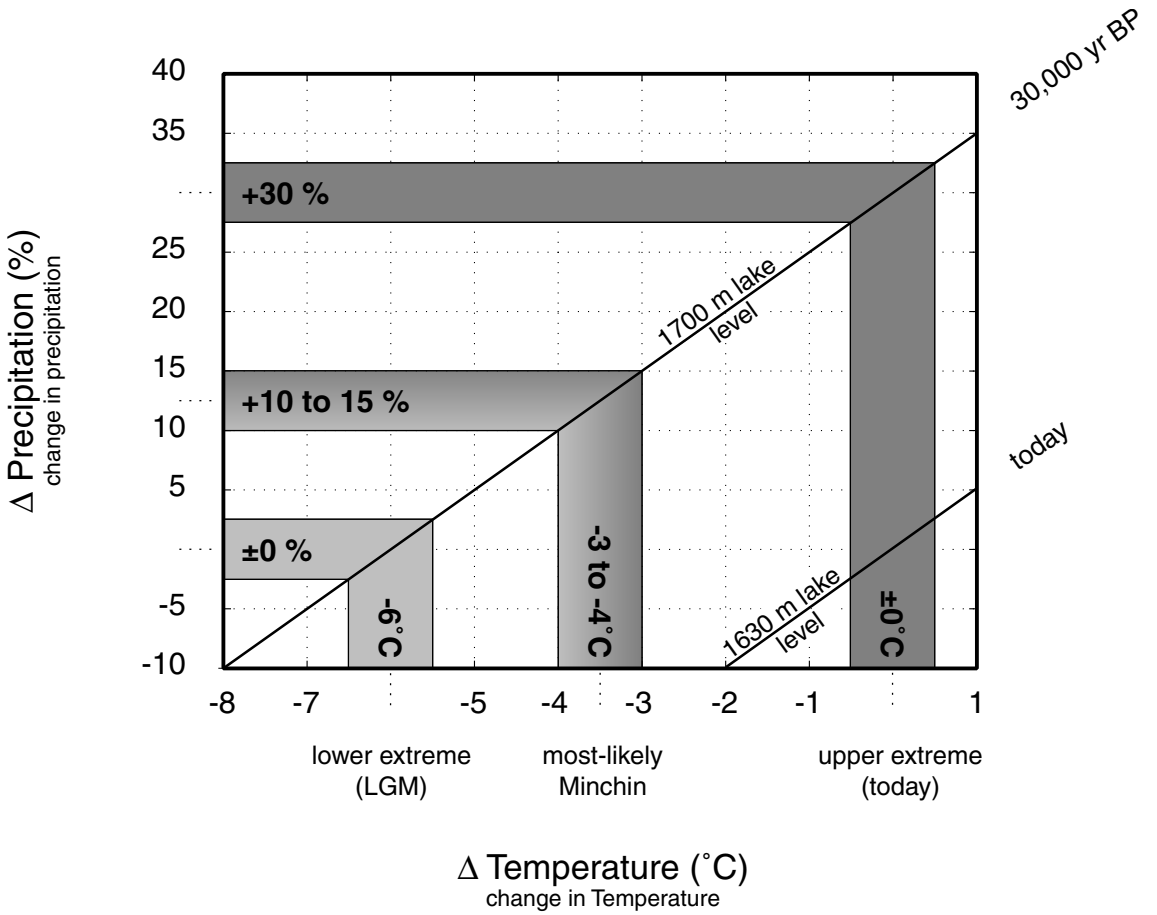

Fig. 8. Potential $\Delta P - \Delta T$-scenarios causing a hypothetical lake at the 1700 m contour. Assuming the present-day mean-annual temperature, an increase in precipitation by 30% would be necessary to cause a lake as reconstructed from the 30,000 ^{14}C yr BP old sediment. As the other extreme, LGM temperatures ($\Delta T = -6$°C) would cause a similar lake without any precipitation change. For intermediate Minchin conditions ($\Delta T = -3$°C to -4°C), the corresponding precipitation increase would be 10–15%.

of $T_s = 20.4$°C measured in the town of Cafayate (van Wambeke, 1981). Basin geometry as given by the hypsometric integral shows that a high percentage of land area has elevation within 100 m of the elevation of Cafayate. The calculated mean annual T_s is only slightly lower because of that small percentage of the catchment area at a higher elevation and therefore lower temperature. However, the agreement of real and modelled data shows that reasonable temperatures are derived in the model.

As a fourth quality check of the result, the modelled evaporation rate E is compared to the difference between real discharge data D from a station in the vicinity of the landslide deposits (Malamud et al., 1996) and precipitation data P (Bianchi and Yañez, 1992) using $E = P \times (1 - \lambda) - D$, where λ is the runoff coefficient reflecting precipitation loss to the ground. The stream flow at the catchment outlet integrates all processes taking place within the catchment including atmospheric processes which impact upon it. Thus stream flow is usually the first and often the only measure, which is available for testing the performance of a hydrologic model. For the Santa Maria Basin, the runoff coefficient λ is calculated as to be $\lambda = 0.017$, which is consistent with the empirical value of $\lambda < 0.1$ for arid environments (Rowntree, 1988).

Summarizing the sensitivity tests, the model yields

reasonable results with realistic values for all parameters without reacting over sensitively to any variable. This suggests that it is a valuable tool for modelling the hydrologic budget for both present and paleo-conditions in the Santa Maria Basin.

6. Modelling Results

The model was applied to two different climate scenarios: first a hypothetical modern lake and second environmental conditions at 30,000 ^{14}C yr BP (Fig. 7). The asymptotic approach to equilibrium lake level (shown in Fig. 7) illustrates the increasing basin-wide evaporation as the lake level rises and hence the area covered by water grows (evaporation over water being greater than over land). Applying parameters for present-day climate, the model results in an equilibrium lake level at 1630 m a.s.l., assuming closure of the valley at the same position as the paleo-landslide in the Quebrada de Cafayate. This hypothetical lake would have an area of 379 km^2 and a volume of 23 km^3. The fill-up time to reach the equilibrium level is 250 yr. In contrast, the paleolake as reconstructed from remnant lake deposits covered an area of 658 km^3 with a volume of 62 km^3. In order to reach this paleolake level, substantial changes of the input parameters have been introduced to the model. Two end-member scenarios illustrate the range of potential paleoclimate conditions that could have caused a lake up to the 1700 m contour. Assuming no change in the mean-annual precipitation, a temperature reduction of 6°C would be necessary. Alternatively, 30% more precipitation results in a similar water budget if the temperature would be at the modern value. In both cases, the equilibrium lake level would reach the 1700 m contour within 400 yr. Again, emphasizing that those are only minimum modelling results, the actual precipitation and temperature increase could be even more significant.

7. Paleoclimatic implications

The enormous discrepancy between the reconstructed lake volume 30,000 ^{14}C yr ago and the hypothetical water body today suggest significant differences in climate. Sensitivity testing of the lake-balance model indicate that the critical climate parameters are temperature T and precipitation P. A potential range for these parameters can be indicated by the climate conditions during the Last Glacial Maximum (LGM) and the modern climate (Fig. 8). During the LGM, mean annual temperatures were reduced by 5–7.5°C as inferred from snowline depressions and the atmospheric lapse rate (Klein, 1996). The comparison between past and modern snowline distributions suggests consistent easterly and northeasterly sources of moisture during the Late Pleistocene (Fox and Strecker, 1991; Klein, 1996). Assuming a 5–7.5°C decrease in temperature, no precipitation change compared to the present would be necessary to generate a lake as reconstructed from the 30,000 ^{14}C yr old sediments. However, no such large landslides are reported for either the LGM or at present. This suggests that the modern mean-annual precipitation is well below the threshold for landslide generation. A higher mean annual average precipitation might also be accompanied by more extreme events, which are then potential landslide triggers.

The other end-member for the realistic temperature range is the present-day conditions. Assuming no temperature change from the modern value, an increase of 30% in precipitation would be necessary to cause a stable lake at 1700 m. Since a precipitation increase without a temperature drop seems very unlikely, a carefully combination of both climatic parameters has been chosen.

For the Minchin wet period between 40,000 and 25,000 ^{14}C yr BP, no temperature reconstructions are available for NW Argentina. However, further to the south (42°S), Markgraf et al. assumes a moderate temperature reduction of 3–4°C compared to the present for this time period (Markgraf et al., 1986; Markgraf, 1989). The corresponding precipitation increase in order to reach the 1700 m contour for the paleolake as inferred from the modelling results is 10–15%.

This paleo-climate scenario is within the expected range for T and P for Minchin times. Higher precipitation in the tropical and subtropical Andes 30,000 ^{14}C yr ago is also indicated by the larger paleolakes Titicaca and Poopo on the Altiplano (Wirrmann and Mourguiart, 1995). Just like the lakes on this plateau glacial meltwater cannot account for paleolake expansion in the Santa Maria Basin, since only sparse

glaciation occurred in the catchment area. Since we conclude that the landslide dam caused a closed-basin lake without discharge, the main variables in the water budget are precipitation and evaporation. The Minchin wet period now possibly characterized by a minimum increase in rainfall of 10–15% in NW Argentina corresponds to a period of enhanced landsliding in narrow valleys and basins in this region (Trauth and Strecker, 1999). More precipitation and runoff could have caused more scouring at the mountain fronts with high relief contrasts, partly preconditioned by intense jointing and faulting (Trauth et al., 2000; Strecker and Marrett, 1999).

One question is whether an increase in precipitation and runoff by 10–15% is enough to reduce the threshold for landsliding in this region. The Minchin phase is also a period of strong El Niño/Southern Oscillation (ENSO) influence (Oberhänsli et al., 1990; Trauth and Strecker, 1999). Heavy rainfall events and higher fluctuations in river discharge caused by extreme ENSO events are an alternative explanation for mass movements as reported from other Andean regions (Grosjean et al., 1997; Keefer et al., 1998; Strecker and Marrett, 1999; Hermanns and Strecker, 1999). A higher mean-annual precipitation could be accompanied by a higher intensity of rainfall during extreme events, which are the actual triggers for releasing landslides (Dethier and Reneau, 1996; Keefer et al., 1998). From the modelling results it cannot be concluded if an increase in mean-annual precipitation by 10–15% can explain enhanced landsliding in NW Argentina or if heavy ENSO-related rainfall events are more effective in preconditioning mountain fronts to failure. In this context, lake-balance modelling for other landslide-dammed paleolakes in the region as well as high-resolution reconstructions of the climate dynamics from varved lake sediments could help to judge the role of higher moisture levels and increased precipitation variability for the generation of catastrophic mass movements in mountainous regions.

Acknowledgements

This work is part of the Collaborative Research Center 267 'Deformation Processes in the Andes' supported by the German Research Foundation. The success of this project was made possible through the support of many Argentine friends and colleagues, with particulary thanks to R. Alonso and J.A. Salfity. We also gratefully acknowledge M. Strecker for his support and discussions of the manuscript. We thank the journal editor as well as D. Dethier and a anonymous reviewer for their comments on the manuscript.

References

Berger, A., Loutre, M.F., 1991. Insolation values for the climate of the last 10 million years. Quaternary Sciences Review 10 (4), 297–317.

Bianchi, A.F., Yañez, C.E., 1992. Las precipitaciones en el noroeste Argentino, Segunda Edicion, Instituto nacional de tecnologia agropecuaria estacion experimental agropecuaria Salta.

Blodgett, T.A., Lenters, J.D., Isacks, B.L., 1997. Constraints on the origin of paleolake expansions in the Central Andes. Earth Interactions 1 (Available online athttp://EarthInteractions.org.).

Bougeault, P., 1988. Evaporation models in hydrology. In: Schmugge, T.J., André, J. (Eds.). Land Surface Evaporation — Measurement and Parameterization. Springer, New York, pp. 93–120.

Brutsaert, W., 1982. Evaporation into the Atmosphere. Reidel, Dordrecht.

Dethier, D.P., Reneau, S.L., 1996. Lacustrine chronolgy links late Pleistocene climate change and mass movement in northern New Mexico. Geology 24, 539–542.

Fox, A.N., Strecker, M.R., 1991. Pleistocene and modern snowlines in the Central Andes (24–28°S). Bamberger Geographische Schriften 11, 169–182.

Galvan, A.F., 1981. Descripcion geológica de la Hoja 10 e Cafayate (Provincias de Tucumán, Salta y Catamarca). Boletín, Servicio Geológica Nacional, 177.

Grosjean, M., Núñez, L., Cartajena, I., Messerli, B., 1997. Mid-Holocene climate and culture change in the Atacama desert Northern Chile. Quaternary Research 48, 239–246.

van der Hammen, T., Absy, M.L., 1994. Amazonia during the last glacial. Palaeogeography, Palaeoclimatology, Palaeoecology 109, 247–261.

Hartmann, D.L., 1994. Global Physical Climatology. Academic Press, San Diego.

Hastenrath, S., 1991. Climate Dynamics of the Tropics. Kluwer Academic Publishers, Dortrecht.

Hastenrath, S., Kutzbach, J., 1985. Late Pleistocene climate and water budget of the South American Altiplano. Quaternary Research 24, 249–256.

Hermanns, R.L., Strecker, M.R., 1999. Structural and lithological controls on large Quaternary rock avalanches (sturzstroms) in arid north-western Argentina. GSA Bulletin 111 (6), 934–948.

Hermanns, R.L., Trauth, M.H., Niedermann, S., McWilliams, M., Strecker, M.R., 2000. Tephrochronologic constraints on the temporal distribution of large landslides in NW Argentina. Journal of Geology, 8.

Hoffmann, J.A.J., 1975. Climatic Atlas of South America — Maps

of Mean Temperature and Precipitation. WMO, Unesco Cartographia.

Imberger, J., Patterson, J.C., 1990. Physical limnology. Advances in Applied Mechanics 27, 303–475.

Kessler, A., 1984. The paleohydrology of the Late Pleistocene Lake Tauca on the southern Altiplano (Bolivia) and recent climatic fluctuations. SASQUA International Symposium, Swaziland, pp. 115–122.

Keefer, D.K., deFrance, S.D., Moseley, M.D., Richardson III, J.B., Satterlee, D.R., Day-Lewis, A., 1998. Early maritime economy and El Niño events at Quebrada Tacahuay, Peru. Science 281, 1833–1835.

Klein, A.G., Isacks, B.L., Bloom, A.L., 1996. Modern and last glacial maximum snowline in Peru and Bolivia: implications for regional climatic change. Bulletin de L'Institut Francais D'Etudes Andines 24, 1–11.

Ledru, M.P., Braga, P.I.S., Soubiès, F., Fournier, M., Martin, L., Suguio, K., Turcq, B., 1996. The last 50,000 years in the Neotropics (Southern Brazil): evolution of vegetation and climate. Palaeogeography, Palaeoclimatology, Palaeoecology 123, 239–257.

Lenters, J.D., Cook, K.H., 1999. Summertime precipitation variability over South America: role of the large-scale circulation. Monthly Weather Review 127, 409–431.

Malamud, B.D., Jordan, T.E., Alonso, R.A., Gallardo, E.F., González, R.E., Kelley, S.A., 1996. Pleistocene Lake Lerma, Salta Province, NW Argentina, XIII Congreso Geológico Argentino y II Congreso de Exploración de Hidrocarburos, ActasIV, pp. 103–114.

Markgraf, V., 1989. Palaeoclimates in Central and South America since 18,000 BP based on pollen and lake-level records. Quaternary Science Reviews 8, 1–24.

Markgraf, V., Bradbury, J.P., Fernandez, J., 1986. Bajada de Rahue, Province of Neuquen, Argentina: an interstadial deposit in northern Patagonia. Palaeogeography, Palaeoclimatology, Palaeoecology 56, 251–258.

Oberhänsli, H., Heinze, P., Diester-Haass, L., Wefer, G., 1990. Upwelling off Peru during the last 430,000 yr and its relationship to the bottom-water environment, as deduced from coarse grain-size distributions and analyses of benthic foraminifers at Holes 679D, 680B, and 681B, Leg 112. Proceedings of the Ocean Drilling Program, Scientific Results 112, 369–391.

Prohaska, F., 1976. The climate of Argentina Paraguay and Uruguay. World Survey of Climatology — Climates of Central and South America 12, 13–112.

Reneau, S.L., Dethier, D.P., 1996. Late Pleistocene landslide-dammed lakes along the Rio Grande, White Rock Canyon, New Mexico. GSA Bulletin 108, 1492–1507.

Rowntree, P.R., 1988. Atmospheric parameterization schemes for evaporation over land: basic concepts and climate modeling aspects. In: Schmugge, T.J., André, J. (Eds.). Land Surface Evaporation — Measurement and Parameterization. Springer, New York, pp. 5–29.

Shuttleworth, W.J., 1988. Parameterization schemes of land-surface processes for mesoscale atmospheric models. In: Schmugge, T.J., André, J. (Eds.). Land Surface Evaporation — Measurement and Parameterization. Springer, New York, pp. 55–92.

Shuttleworth, W.J., 1993. In: Maidment, D.R. (Ed.). Evapotranspiration, Handbook of Hydrology. McGraw-Hill, New York.

Strecker, M.R., Marrett, R., 1999. Kinematic evolution of fault ramps and its role in development of landslides and lakes in the northwestern Argentine Andes. Geology 27, 307–310.

Tineo, A., Ivaldi, E.F., 1993. Caracteristicas Hidrogeologicas del Valle del Rio Santa Maria, Provincia de Tucuman, XII Congreso Geologico Argentino y il Congreso de Exploracion de Hidrocarburos, Actas VI, pp. 166–171.

Trauth, M.H., Strecker, M.R., 1999. Formation of landslide-dammed lakes during a wet period between 40,000 and 25,000 yr BP in northwestern Argentina. Palaeogeography, Palaeoclimatology, Palaeoecology 153, 277–287.

Trauth, M.H., Alonso, R., Strecker, M.R., 2000. Formation of landslide-dammed lakes during a wet period between 40,000 and 25,000 yr BP in northwestern Argentina. EPSL 153, 277–287.

Turcq, B., Pressinotti, M.M.N., Martin, L., 1997. Paleohydrology and Paleoclimate of the past 33,000 Years at the Tamaduà River, Central Brazil. Quaternary Research 47, 284–294.

van Wambeke, A., 1981. Calculated soil moisture and temperature regimes of South America, Soil Management Support Service (SMSS).

Wessel, P., Bercovici, D., 1998. Interpolation with splines in tension: a green's function approach. Mathematical Geology 30, 77–93.

Wirrmann, D., Mourguiart, P., 1995. Late Quaternary spatiotemporal limnological variations in the Altiplano of Boliva and Peru. Quaternary Research 43, 344–354.